STIC-ILL

From: Brunovskis, Peter
Sent: Thursday, February 24, 2000 8:54 PM
To: STIC-ILL
Subject: references needed

Please forward me the following references:

1) Kirkpatrick, Cell. Mol. Life Sci., 55(3):437-449 (March 1999).
2) Kolodner and Marsischky, Curr Opin. Genet. Dev., 9(1):89-96 (Feb. 1999).
3) Chamber et al., Mol. Cell. Biol., 16(11):6110-6120 (Nov. 1996).
4) Hunter et al., EMBO J., 15(7):1726-1733 (April 1, 1996).
5) Richardson et al., Biol. Reprod., 62(3):789-796 (March 2000).
6) Baker et al., Nat. Genet., 13(3):336-342 (July 1996).
7) Hassold, Nat. Genet., 13(3):261-262 (July 1996).
8) Datta et al., PNAS, 94(18):9757-9762 (Sept. 2, 1997).
9) Hunter and Borts, Genes Dev., 11(12):1573-1582 (Jun. 15, 1997).
10) Sniegowski, Curr. Biol., 8(2):R59-61 (Jan. 15, 1998).
11) Jiricny, Mutat. Res., 409(3):107-121 (Dec. 14, 1998).
12) Yamazaki et al., J. Exp. Zool., 286(2):212-218 (Feb. 1, 2000).
13) Prelle et al., Cells Tissues Organs, 165(3-4):220-236 (1999).

Thanks in advance,

Peter Brunovskis
Art Unit 1632
CM1-Rm 12E05
305-2471

Involvement of mouse *Mlh1* in DNA mismatch repair and meiotic crossing over

Sean M. Baker[1*], Annemieke W. Plug[2*], Tomas A. Prolla[3], C. Eric Bronner[1], Allie C. Harris[1], Xiang Yao[4], Donna-Marie Christie[1], Craig Monell[5], Norm Arnheim[4], Allan Bradley[3], Terry Ashley[2] & R. Michael Liskay[1]

Mice that are deficient in either the *Pms2* or *Msh2* DNA mismatch repair genes have microsatellite instability and a predisposition to tumours. Interestingly, *Pms2*-deficient males display sterility associated with abnormal chromosome pairing in meiosis. Here mice deficient in another mismatch repair gene, *Mlh1*, possess not only microsatellite instability but are also infertile (both males and females). *Mlh1*-deficient spermatocytes exhibit high levels of prematurely separated chromosomes and arrest in first division meiosis. We also show that Mlh1 appears to localize to sites of crossing over on meiotic chromosomes. Together these findings suggest that *Mlh1* is involved in DNA mismatch repair and meiotic crossing over.

[1]*Department of Molecular and Medical Genetics, L103, Oregon Health Sciences University, 3181 S. W. Sam Jackson Park Road, Portland, Oregon 97201-3098, USA*
[2]*Department of Genetics, Yale University School of Medicine, 333 Cedar Street, New Haven, Connecticut 06510, USA*
[3]*Department of Molecular and Human Genetics, Howard Hughes Medical Institute, Baylor College of Medicine, Houston, Texas 77030, USA*
[4]*Molecular Biology Program, University of Southern California, Los Angeles, California 90089-1340, USA*
[5]*PharMingen, 10975 Torreyana Rd. San Diego, California 92121, USA*

**S.M.B. & A.W.P. contributed equally to this study*

Correspondence should be addressed to R.M.L. e-mail: liskaym@ohsu.edu

DNA mismatch repair plays a prominent role in the correction of replicative mismatches which escape DNA polymerase proof-reading, mismatches that arise due to spontaneous deamination of 5-methylcytosine, and mispairs that form during genetic recombination[1]. Three genes, *mutS*, *mutL* and *mutH* are central to the correction of replication errors in *Escherichia coli*[1]. Biochemical studies indicate that the MutS protein recognizes DNA mismatches and that the MutH protein is an endonuclease that helps direct repair to newly synthesized strands[1,2]. The MutL protein appears to couple mismatch recognition by MutS to MutH activation[2].

Multiple genes with roles in DNA mismatch repair have been identified in the yeast *Saccharomyces cerevisiae* and in mammals[3–10]. Genetic analysis in yeast has identified three *mutS* homologues, *MSH2* (ref. 3), *MSH3* (ref. 11) and *MSH6* (ref. 12), and two *mutL* homologues, *PMS1* and *MLH1* (refs 4,5,13,14) that appear to function as components of the same replicative DNA mismatch repair pathway. Recent studies suggest that early steps in yeast mismatch repair include recognition of mispaired bases by a heterodimer of MSH2 and either MSH3, or MSH6 (ref. 12) followed by binding of a heterodimer of MLH1 and PMS1 (ref. 15). In humans, mutation in the *mutS* homologue, *MSH2* (refs 7,8), or in any of three *mutL* homologues, *PMS2*, *PMS1* and *MLH1* (refs 6,9,10), is associated with hereditary colorectal cancer. Mice engineered to be deficient in either *Pms2* (the homologue of yeast *PMS1*) or *Msh2* show microsatellite instability and predisposition to early onset cancers, primarily lymphomas[16–18]. The conservation of eukaryotic DNA mismatch repair mechanisms is suggested by biochemical studies that indicate the human MSH2 protein can bind mispaired DNA[19], and that human MLH1 and PMS2 can exist as a heterodimer (ref. 20; A.B. Buermeyer & R.M.L., unpublished observations).

In addition to reducing mutations, DNA mismatch repair appears to play several roles in genetic recombination[21–24], including the correction of heteroduplex DNA[21] and the regulation of recombination between similar but non identical DNA sequences[25–28]. Moreover, specific DNA mismatch repair gene homologues are involved in different aspects of recombination. For example, the yeast *mutS* homologues, *MSH4* and *MSH5*, each play a part in meiotic crossing over but not DNA mismatch repair[29,30]. In contrast, yeast *PMS1*

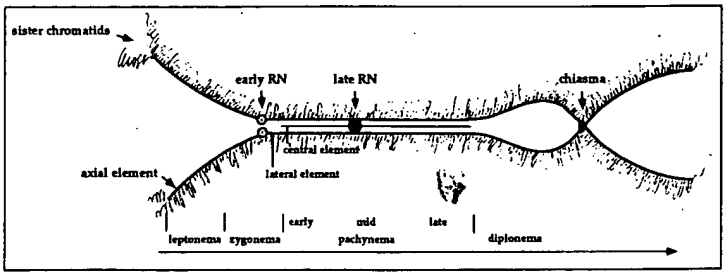

Fig. 1 Meiotic prophase in mammals, showing a timeline of meiotic-specific structural components.

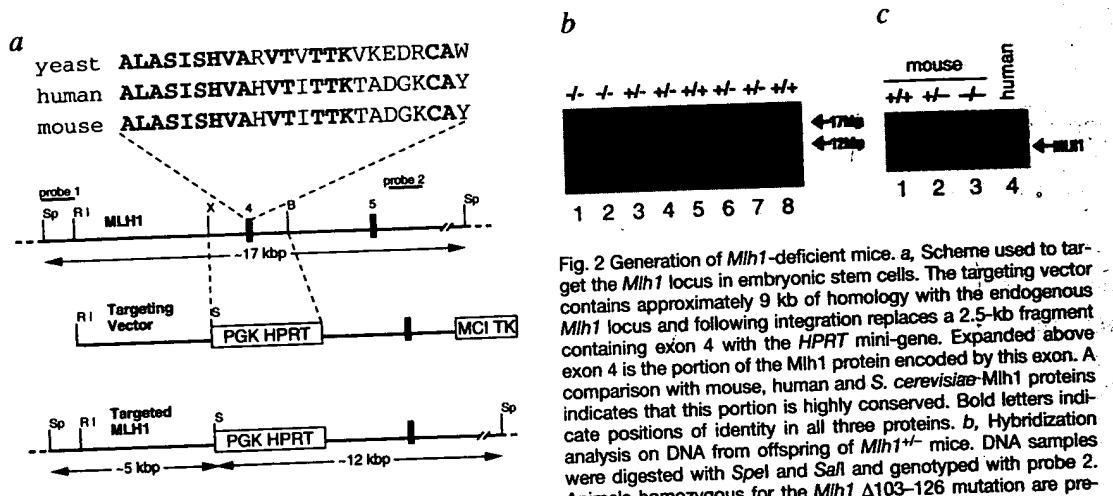

Fig. 2 Generation of *Mlh1*-deficient mice. *a*, Scheme used to target the *Mlh1* locus in embryonic stem cells. The targeting vector contains approximately 9 kb of homology with the endogenous *Mlh1* locus and following integration replaces a 2.5-kb fragment containing exon 4 with the *HPRT* mini-gene. Expanded above exon 4 is the portion of the Mlh1 protein encoded by this exon. A comparison with mouse, human and *S. cerevisiae* Mlh1 proteins indicates that this portion is highly conserved. Bold letters indicate positions of identity in all three proteins. *b*, Hybridization analysis on DNA from offspring of $Mlh1^{+/-}$ mice. DNA samples were digested with *Spe*I and *Sal*I and genotyped with probe 2. Animals homozygous for the *Mlh1* Δ103–126 mutation are present in lanes 1 and 2. $Mlh1^{+/+}$ (lanes 5, 8) and $Mlh1^{+/-}$ (lanes 3, 4, 6, 7) animals were also identified. The genotypes have been confirmed by PCR (see Methods). *c*, Immunoblot analysis on extracts from mouse $Mlh1^{+/+}$, $Mlh1^{+/-}$ and $Mlh1^{-/-}$ fibroblasts cells. Mlh1 protein can be detected in the $Mlh1^{+/+}$ (lane 1) and $Mlh1^{+/-}$ (lane 2) cell extracts, but not in extracts from $Mlh1^{-/-}$ cells (lane 3).

is involved in DNA mismatch repair but not meiotic crossing over[14]. Therefore, mismatch repair deficiency in mammals might affect meiotic events such as crossing over, or chromosome pairing. In fact, *Pms2*-deficiency in the mouse results in male infertility associated with the disruption of normal chromosome synapsis (pairing) during meiosis[16].

In most eukaryotes, synapsis and crossing over of homologous chromosomes are critical for the basic function of meiosis: to segregate a complete haploid set of chromosomes to each gamete. Proper segregation of homologues in first division meiosis requires that they are held together by chiasmata to ensure correct chromosomal alignment at metaphase I[31,32]. Chiasmata represent the physical manifestations of crossing over, or reciprocal recombination, and are first detected cytologically when homologues begin to separate at diplonema (Fig. 1). However, studies on diverse organisms suggest that crossing over occurs earlier in prophase, during pachynema, within electron dense structures on the synaptonemal complex (SC) termed late recombination nodules (late RNs). The number and distribution of late RNs correlate well with crossover events in microorganisms, insects and plants[33] but not in mammals[34]. Although RNs are assumed to represent recombination protein complexes, specific components of RNs have not been identified.

To define the role of *Mlh1* in mice we have taken two complementary approaches. First, we have derived mice defective in *Mlh1* function and second, we have localized Mlh1 protein in male and female meiotic nuclei. Here we report that in addition to compromising replication fidelity, *Mlh1*-deficiency appears to cause both male and female sterility associated with reduced levels of chiasmata. Significantly, we find that Mlh1 protein appears to be present at sites of interhomologue crossing over and chiasma formation in normal spermatocytes and oocytes. Our findings suggest roles for mouse *Mlh1* in both DNA mismatch repair and meiotic crossing over.

Generation and analysis of *Mlh1*-deficient mice

We used a portion of the human *MLH1* cDNA[6] as a probe to isolate mouse *Mlh1* cDNA and genomic clones. To generate mice with a null mutation in *Mlh1*, we transfected a replacement vector (Fig. 2*a*) into mouse embryonic stem (ES) cells to delete by homologous recombination an exon encoding a highly conserved region (Fig. 2*a*) of the mouse Mlh1 protein. Targeted ES cell clones were identified by hybridization with probes 5' and 3' (Fig. 2*a*) to the targeted region (data not shown), and injected into host blastocysts to generate chimaeric animals that transmitted the *Mlh1* mutant allele (Δ103–126 mutation) to F1 offspring (Fig. 2*b*). Of 145 offspring from $Mlh1^{+/-}$ intercrosses, 10% were $Mlh1^{+/+}$, 65% $Mlh1^{+/-}$ and 25% $Mlh1^{-/-}$, suggesting that *Mlh1* function is not essential for normal somatic development.

To determine the consequence of the Δ103–126 mutation on Mlh1 protein expression, we used a monoclonal antibody raised against human MLH1 for immunoblot analysis of $Mlh1^{+/+}$, $Mlh1^{+/-}$ and $Mlh1^{-/-}$ fibroblast cells extracts. Consistent with a null mutation, we detected no normal-length Mlh1 in the $Mlh1^{-/-}$ cell extract (Fig. 2*c*). To determine the consequence of *Mlh1* disruption on mismatch repair, we measured mutation in $(CA)_n$ microsatellite repeats using single molecule dilution PCR on spleen DNA samples from $Mlh1^{+/+}$ and $Mlh1^{-/-}$ animals[35]. *Mlh1*-deficiency resulted in an elevated level of CA-repeat mutation in spleen DNA (Table 1). Studies on germ cell enriched samples taken from seminiferous tubules demonstrated that *Mlh1*-deficiency also destabilized simple sequence repeats in the male germ line (Table 1). The elevated mutation level in enriched spermatocytes may represent either mitotic instability, meiotic instability, or both. Preliminary experiments with cultured cell lines from *Mlh1*-deficient mice show an increased rate of mutation to oubain resistance, suggesting that the role for *Mlh1* in replicative fidelity is not limited to microsatellite sequences (C.E.B. & R.M.L., unpublished observation). Furthermore, consistent with the cancer predisposition seen in *Pms2*- and *Msh2*-knockout mice[16–18], an *Mlh1*-deficient female, sacrificed at six months of age for ovarian analysis, had developed a lymphoma.

Table 1 Microsatellite mutation in normal and *Mlh1*-deficient mice

DNA	Locus *D9Mit67*	Locus *D1Mit355*
Mlh1$^{+/+}$ Spleen	0/103 (0%)	3/131 (2.3%)
Mlh1$^{-/-}$ Spleen	42/221 (19%)	50/246 (20.3%)
[a]*Mlh1*$^{+/+}$ Sperm	0/136 (0%)	not tested
Mlh1$^{-/-}$ Spermatocytes	32/229 (14%)	33/180 (18.3%)

The number of DNA samples with altered microsatellite sequences divided by the total number of samples examined for each locus. Purified DNA was diluted so that one third of the samples gave a PCR product. The data were obtained through analysis of a single animal of each genotype. The *Mlh1*$^{-/-}$ animal was heterozygous for the C57BL/6 and 129 alleles at each locus. At *D9Mit67*, we estimate that the alleles differ by 6 (CA/GT) repeats and at *D1Mit355* by 7 repeats. In the *Mlh1*$^{-/-}$ mouse, length alterations were observed equally among the C57BL/6 and 129 alleles. At each locus we observed approximately twice as many contractions as expansions, primarily one or two repeats. [a]We reported this data for wild-type sperm previously[16].

Gonadal analysis of *Mlh1*-deficient animals

To determine the effect of *Mlh1*-deficiency on the male germline, we examined the contents of the caudal epididymis and testes from *Mlh1*$^{+/-}$ and *Mlh1*$^{-/-}$ animals. Whereas the epididymis from *Mlh1*$^{+/-}$ animals contained normal spermatozoa, we observed no spermatozoa in three *Mlh1*$^{-/-}$ animals. Histological sectioning of testes from *Mlh1*$^{-/-}$ animals revealed abnormal spermatogenesis, the most notable phenotype being an absence of late stage cells—round spermatids through spermatozoa (Fig. 3*a*,*b*). There was a clear excess of primary spermatocytes, many with condensed chromosomes, consistent with meiosis I arrest in late pachynema, metaphase, or both. Although not directly tested, the total absence of spermatozoa in the *Mlh1*$^{-/-}$ mice predicts that *Mlh1*-deficiency result in male infertility.

Matings of *Mlh1*$^{+/-}$ females with *Mlh1*$^{+/-}$ males produced litters of normal size (data not shown). However, matings involving *Mlh1*$^{-/-}$ females were unsuccessful, suggesting that these females were infertile. Histological sections showed that ovaries from *Mlh1*-deficient adult females (Fig. 3*d*) were clearly smaller than wild-type (Fig. 3*c*), had very few follicles and showed an increased proportion of stromal cells. Nonetheless, we observed a reduced number of corpora lutea suggesting that ovulation can occur in the *Mlh1*-deficient females, albeit infrequently.

A meiotic defect in *Mlh1*-deficient males

The excess of primary spermatocytes and lack of spermatids in the *Mlh1*-deficient males suggested a meiosis I arrest. Therefore, we examined meiotic progression in *Mlh1*-deficient spermatocytes using both standard DAPI staining and immunostaining with Rad51 antibody[36]. One of the several positive reactions of this polyclonal antibody is the staining of axial (unsynapsed)/lateral (synapsed) elements of the SCs. This reaction, along with the two types of Rad51 foci, provides cytological landmarks for meiotic prophase from leptonema, prior to homologue synapsis, through axial disassembly as homologues begin to separate at diakinesis (see Fig. 1). Rad51-staining revealed that chromosome pairing behavior in the zygotene through early pachytene stages of prophase I was normal in *Mlh1*-deficient spermatocytes (data not shown). We did not observe the synaptic abnormalities reported for *Pms2*-deficient spermatocytes[16]. By mid-pachynema in normal mice, the X and Y chromosomes begin to desynapse, although they remain held together at their distal ends, presumably by a chiasma[26,37–41] in the psuedoautosomal region (Fig. 4*a*). In contrast, by mid-pachynema in *Mlh1*-deficient nuclei, the X and Y were completely separated, giving rise to X and Y univalents (Fig. 4*b*). The autosomes in both wild-type and *Mlh1*$^{-/-}$ nuclei remained fully synapsed throughout pachynema (Fig. 4*a*, *b*). As homologues desynapse in normal diplonema, the bivalents remained connected at the sites of chiasmata (Fig. 4*c*). In contrast, as desynapsis of the autosomes progressed in *Mlh1*$^{-/-}$ diplotene nuclei, we observed a steady increase in the frequency of univalents (Fig. 4*d*). By metaphase I, homologous autosomes of wild-type mice remained connected by chiasmata (Fig. 4*e*), whereas in *Mlh1*-deficient nuclei we observed primarily univalents, or unassociated homologues (Fig. 4*f*). Examination of multiple diplotene and metaphase nuclei indicated that chiasma formation in *Mlh1*-defi-

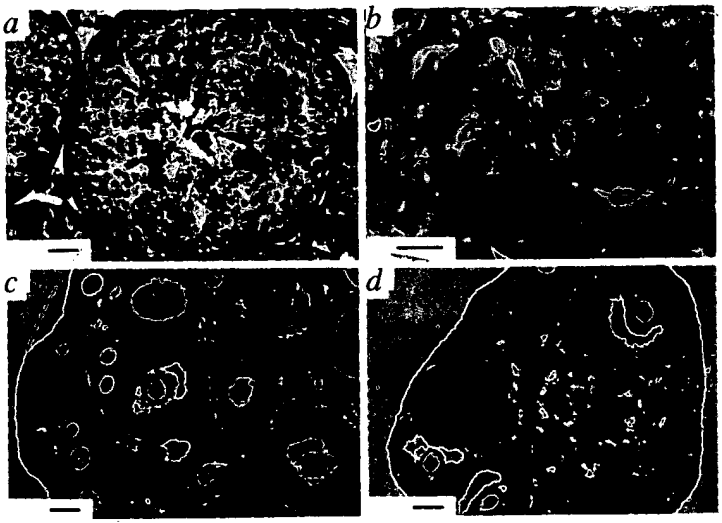

Fig. 3 Testicular and ovarian histology from *Mlh1*$^{+/-}$ and *Mlh1*$^{-/-}$ mice. Cross section through *Mlh1*$^{+/-}$ (*a*) and *Mlh1*$^{-/-}$ (*b*) seminiferous tubules, stained with periodic acid, Schiff's and haematoxylin. Spermatogenesis is normal in the *Mlh1*$^{+/-}$ tubules (*a*) as indicated by the production of mature spermatozoa and the appropriate proportion of cells in each sub-stage. In *Mlh1*$^{-/-}$ tubules (*b*), there is an accumulation of primary spermatocytes and an absence of late stage cells, round spermatids through spermatozoa. The later stages of spermatogenesis are absent from all tubules. Bar in (*a*) and (*b*) is 25 μm in length. Histology of *Mlh1*$^{+/-}$ (*c*) and *Mlh1*$^{-/-}$ (*d*) ovaries stained with eosin and haematoxylin. Note the smaller ovary size and the reduced number of follicles in the mutant (*d*) as compared to the *Mlh1*$^{+/-}$ ovary (*c*). Bar in (*c*) and (*d*) is 100 μm in length.

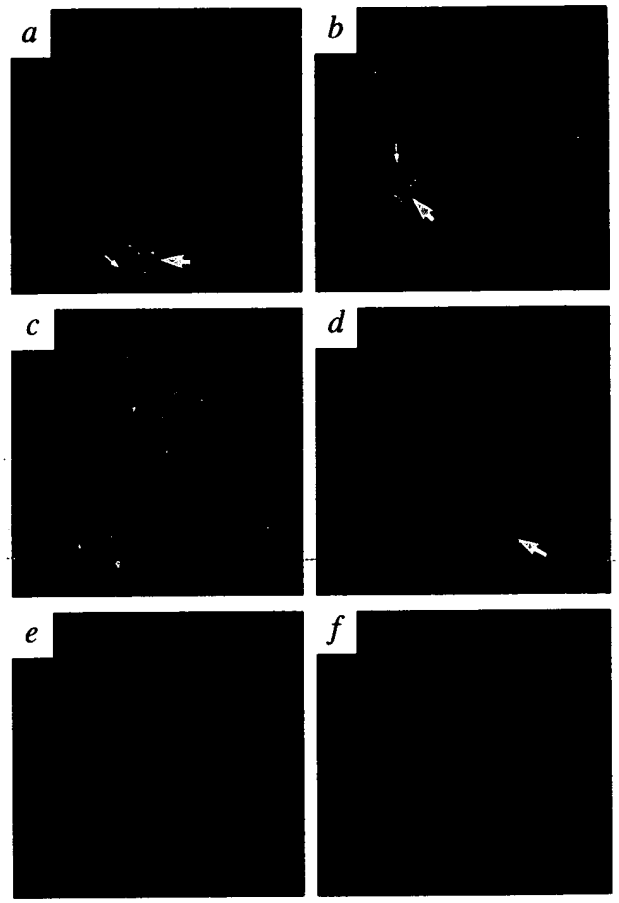

Fig. 4. Analysis of primary spermatocytes from *Mlh1*$^{-/-}$ and *Mlh1*$^{+/+}$ mice. Spermatocytes were stained with human Rad51 antibody (panels *a–d*). Left panels represent normal mice, right panels, *Mlh1*$^{-/-}$ mice. *a,b*, Pachytene. *a*, Wild-type nucleus: the X and Y (arrow) have desynapsed, but show end association; *b*, *Mlh1*$^{-/-}$ nucleus: the X (large arrow) and Y (small arrow) chromosomes are completely separated. Synapsis of the autosomes for wild-type and *Mlh1*-deficient nuclei is completely normal. *c*, *d*, Diplotene. *c*, In wild-type nuclei the autosomes show initial desynapsis, and are held together as bivalents (pairs of homologues) by chiasma. *d*, In *Mlh1*$^{-/-}$ nuclei homologue separation results in univalents (large arrows). *e*, *f*, Metaphase stained with DAPI. Brightly staining areas are centromeric heterochromatin. The wild-type nuclei (*e*) contains 20 bivalents; whereas *Mlh1*$^{-/-}$ nuclei (*f*) contain mostly univalents.

cient spermatocytes is reduced 10- to 100-fold. Taken together, these observations suggest that *Mlh1* is required for normal levels of chiasma formation, or stabilization, or both during meiosis I.

Localization of Mlh1 during meiosis

We immunostained surface spread spermatocytes and oocytes from normal mice with an Mlh1 monoclonal antibody and observed discreet fluorescent foci in meiotic prophase nuclei. We observed no Mlh1 foci at any stage of meiotic prophase in spermatocytes from *Mlh1*$^{-/-}$ males indicating that the foci are dependent on Mlh1 and suggesting specificity of the antibody. To provide a temporal and spatial framework for the Mlh1 immunoreactions during meiosis, we used differentially labelled and detected polyclonal antibody[36] directed against human Rad51.

In oocytes from normal females double-stained with the Rad51 and Mlh1 antibodies, we observed Mlh1 foci on synapsed portions of the SC as early as zygonema. By the time the homologues were fully synapsed in early pachynema, there were an average of 65 ± 12 Mlh1 foci per oocyte nucleus ($n = 9$), or 3.25 foci per SC bivalent (Fig. 5*d*). (Mlh1 foci are rapidly lost during this substage, hence the high standard deviation.) The number of foci decreased to an average of 31 ± 2 Mlh1 foci per nucleus ($n = 21$), or 1.5 foci per SC bivalent by mid-pachynema and then stabilized. In spermatocytes, we did not see Mlh1 foci on the SCs until homologues were fully synapsed in early pachynema. The number of Mlh1 foci on the SCs in spermatocytes then increased to average of 22 ± 1.5 foci per nucleus ($n = 29$), or 1.2 foci per autosomal SC bivalent, in mid-pachynema (Fig. 5*a*). In early pachytene spermatocytes, we consistently observed an Mlh1 focus at the distal end of the pairing region of the X and Y (Fig. 5*a*). However, no focus was evident at slightly later substages of pachynema as the X and Y began to desynapse precociously relative to the autosomes (Fig. 5*b*). The number of Mlh1 foci decreased gradually in both oocytes and spermatocytes in late pachynema. In spermatocytes all Mlh1 foci have disappeared by late pachynema. However, in oocytes some Mlh1 foci remain present at sites of chiasmata into early diplonema (Fig. 5*c*).

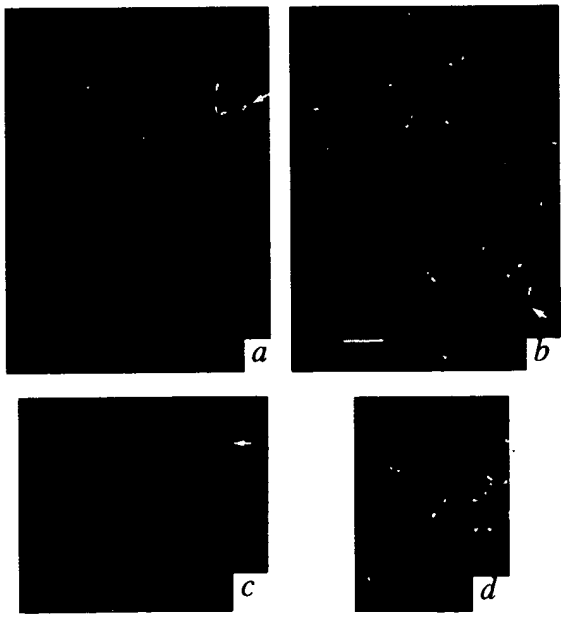

Fig. 5 Double labelling with the polyclonal Rad51 antibody (white) and the monoclonal Mlh1 antibody (red). *a*, Early pachytene spermatocyte- small arrows show Mlh1 foci on SCs, large arrow shows Mlh1 focus at base of the XY pairing region. *b*, Late pachytene spermatocyte. The large arrow identifies an X and Y bivalent without an Mlh1 focus although the number of Mlh1 foci (24) on the autosomal axes at this stage are similar to the number of chiasmata reported for spermatocytes[42]. *c*, Four bivalents from diplotene oocytes. Mlh1 foci remain at some chiasmata sites (arrow). *d*, Bivalents from late zyotene/early pachytene oocytes. Animals were from the inbred strain C57Bl/6.

Discussion

Using gene targeting in ES cells we derived mice deficient in the DNA mismatch repair gene homologue, *Mlh1*. We observed increased mutation in microsatellite DNA sequences in both the spleen and the male

germline of homozygous mutant animals, consistent with a role for *Mlh1* in DNA mismatch repair. The elevated levels of microsatellite mutation in *Mlh1*-deficient mice were similar in degree to the levels previously shown in mice deficient in *Pms2*, another mismatch repair gene[16]. Although the *Mlh1*-deficient mice are at present too young to draw conclusions on cancer susceptibility, the occurrence of a lymphoma in an *Mlh1*-deficient animal is consistent with the tumour-prone phenotype reported for *Pms2*- and *Msh2*-knockout mice[16–18].

A prominent finding was the severe effect that *Mlh1*-deficiency had on both male and female fertility. *Mlh1*-deficient males produced no spermatozoa, while females produced reduced numbers of oocytes and have thus far proven to be functionally sterile. In contrast, *Pms2*-deficient mice exhibited male infertility associated with the production of abnormal spermatozoa but no discernible effect on female fertility[16]. In addition, the spermatogenesis arrest seen in the *Mlh1*-deficient animals was more uniform than that observed for *Pms2* deficiency[16] and suggests a block in first division meiosis.

The abnormal behaviour of homologous chromosomes in *Mlh1*-deficient mice is consistent with reduced levels of chiasmata. Synapsis appeared to proceed normally, in contrast with meiosis in *Pms2*-deficient mice[16]. However, desynapsis at diplonema in *Mlh1*-deficient spermatocytes resulted in complete and premature separation of both the XY pair and the autosomal bivalents. By metaphase I, only univalents were observed suggesting either a failure of homologues to cross over or to maintain chiasmata. In contrast, although we do observe univalents in metaphase *Pms2*-deficient spermatocytes, the degree of univalency is much less than for *Mlh1*-deficiency. The pairing abnormalities associated with *Pms2*-deficiency may be sufficient to account for this degree of univalency. Therefore, in the mouse, Mlh1 appears to be required for normal levels of chiasma formation or stabilization, while Pms2 appears to be required for normal homologue pairing.

In parallel studies, we localized Mlh1 in spermatocytes and oocytes using immunostaining. Four aspects of the localization and timing of Mlh1 provide evidence that the meiotic phenotype of Mlh1-deficiency reflects a direct role of Mlh1 in crossing over. First, despite variation among mouse strains, the total number of Mlh1 foci on the SCs in mid-pachynema in both males and females corresponds to the number of previously reported chiasmata[42] Further, in meiotic analysis of the mouse, a greater number of chiasmata per bivalent were observed in females (in two strains of mice: 1.43 and 1.34 for females; 1.25 and 1.09 for males[42]. Consistent with these studies we observed a comparable difference in the number of Mlh1 foci during mid-pachynema between oocytes and spermatocytes. Second, the timing of stabilization of the number of Mlh1 foci during mid-pachynema in both male and female mice is also consistent with the apparent time of repair DNA synthesis putatively linked to reciprocal recombination[43,44].

Third, Mlh1 was localized at the base of the pairing region of the XY where crossing over is necessary to assure the proper meiotic segregation of the sex chromosomes in most mammalian species[26,37–41]. Further, mammalian sex chromosomes proceed through meiotic prophase out of synchrony with the autosomes; they are the last to synapse and the first to desynapse[45,46]. The timing of the appearance and disappearance of an Mlh1 focus on the XY relative to autosomal foci matches this documented asynchrony and is consistent with the premature separation of the X and Y chromosomes in *Mlh1*-deficient mice.

Fourth, the occurrence of Mlh1 foci at chiasma sites in diplotene oocytes also suggests a direct role for Mlh1 in meiotic crossing over. Although the number of Mlh1 foci at mid-pachynema in oocytes closely corresponds to the previously reported number of chiasmata in diplonema, Mlh1 foci are not present at each chiasma. The absence of Mlh1 at some chiasmata may be due to completion of the Mlh1-dependent step at these locations by the end of pachynema. The disappearance of Mlh1 foci by late pachynema in spermatocytes is also consistent with this interpretation. Pachynema in spermatocytes is prolonged (6 days vs. 3 days in oocytes)[47–50] therefore allowing three extra days for completion of Mlh1-dependent processes before the end of pachynema.

The apparent involvement of Mlh1 in crossing over suggests that Mlh1 may be a component of late RNs, which have been linked to recombination events in mid-to-late pachynema in a variety of organisms[33,51]. However, mammalian studies have consistently reported a deficiency of late RNs relative to the number of chiasmata in late pachytene nuclei, especially in spermatocytes[34]. The comparable drop in RNs[34] and Mlh1 foci between mid and late pachynema in spermatocytes strengthens the supposition that Mlh1 is a component of late RNs. However, the nature of Mlh1 function in reciprocal recombination and the basis for the apparent localization at crossover sites is not clear. Mlh1 may play a role in the formation, stabilization and/or resolution of Holliday-structure intermediates necessary for crossing over[52]. Alternatively, Mlh1 may be an integral part of a multifunctional complex of proteins involved in recombination between homologous chromosomes. Disruption of *Mlh1* could destabilize such a complex, affecting functions in which Mlh1 does not directly participate.

Although we have focused on the clear connections between Mlh1 and crossing over, we note that the number of Mlh1 foci in early pachytene oocytes exceeds the number of expected crossover events. We speculate that these early pachytene Mlh1 foci are associated with recombination intermediates, only some of which ultimately lead to crossing over. Our results do not provide information on the nature of the recombination intermediate that results in localization of Mlh1 to sites of crossing over. However, we suggest that Mlh1 localization does not simply reflect the presence of DNA mispairs, because the use of inbred mice should minimize the potential for such mismatches. In addition, no significant increase in Mlh1 foci was noted in spermatocytes of mice deficient for *Pms2* (unpublished observations), where the associated germline mutator phenotype[16] should have increased the potential for mismatches between homologues. This latter observation also suggests that the

presence of Mlh1 foci is not dependent on the *Pms2* gene product.

Our results show that *Mlh1* in the mouse is involved in both DNA mismatch repair and meiotic crossing over. Whereas our studies show that meiosis in *Mlh1*-deficient spermatocytes is characterized by premature separation of homologues, apparently due to unsuccessful completion of recombination and chiasma formation, a previous study showed that *Pms2* deficiency was associated with synaptic abnormalities[16]. Therefore, the findings reported here and elsewhere[6,9,10,16] indicate that both *Mlh1* and *Pms2* have roles during DNA mismatch repair and meiosis. However, the different meiotic phenotypes of *Pms2* and *Mlh1* mice suggest that these two *MutL* homologues do not fulfill their meiotic functions in concert. Finally, the fertility of *Msh2*-deficient mice raises the possibility that another MutS-like protein, such as homologues of yeast MSH4 or MSH5 (refs 29,30), act in conjunction with Mlh1 and Pms 2 during meiosis. Alternatively, the two MutL homologues might perform their meiotic functions independent of a MutS homologue.

Methods

Isolation of mouse *Mlh1* cDNA. As previously described[6], a 212-bp fragment from the human *Mlh1* was amplified by PCR from human cDNA using degenerate oligonucleotide primers. This human *Mlh1* fragment was used to isolate cDNA clones from a mouse teratocarcinoma cDNA library (λZap, Stratagene). Dideoxy-sequencing was performed according to the manufacturer (United States Biochemical).

Construction of *Mlh1* targeting vector. Using mouse *Mlh1* cDNA, a genomic clone was isolated from a 129/Sv strain library (λFIXII, Stratagene) that contained the first five exons of the open reading frame. The genomic insert was subcloned with *Not*I ends into pBluescript II (SK-) (Stratagene). A 4.7-kb *Bgl*II/*Not*I fragment from the 3' end of the insert was further subcloned into *Bam*HI/*Not*I digested pBluescript. Following digestion with *Sal*I and blunt ending with T4 polymerase, this 3' homology arm for the *Mlh1* targeting vector was cloned into *Bam*HI site (blunted with T4 polymerase), between the *HPRT* minigene and thymidine kinase gene[53]. The 5' homology arm, a 4.5-kb *Eco*RI/*Xba*I fragment, was subcloned into pBluescript. To prepare the insert for cloning into a *Sal*I site 5' of the *HPRT* marker, the clone was first digested with *Xba*I, blunted with T4 polymerase and *Sal*I linkers were ligated. Following digestion with *Sal*I the 5' arm was ligated into the *Sal*I site to generate the *Mlh1* targeting vector.

Targeting of *Mlh1* in mouse ES cells. AB2.2 ES cells were electroporated with *Not*I linearized targeting vector and cultured in HAT medium with FIAU selection[53]. Homologous integration of the targeting construct should introduce an unique *Sal*I restriction site into the *Mlh1* locus. Hybridization analysis[54] of 200 colonies, following digestion with *Spe*I and *Sal*I restriction endonucleases, identified clones which exhibited proper targeting at 5' and 3' ends (Fig. 2).

Generation of *Mlh1*-deficient mice. Blastocyst microinjection, reimplantation, and the generation of chimaeric males with a high (50–90%) contribution of the ES cell-derived (129Sv/Ev strain) Agouti pigmentation to the coat colour was performed as described[55,56]. Southern blot analysis was used to identify $Mlh1^{+/-}$ animals among black agouti offspring of chimaeric males, *Mlh1*-heterozygous siblings were mated to generate $Mlh1^{-/-}$ animals. Subsequent genotyping was performed by PCR using oligonucleotide primers that distinguish the 3' boundary of endogenous and targeted alleles: MLH1-a, AGGAGCTGATGCTGAGGC; MLH1-U, TTTCATCTTGTCACCCGATG; MLH1-T5, GATCTCGACGGTATCGATAAGC. Primers MLH1-a and MLH1-U give a product diagnostic of a untargeted allele that is 258 bp in length, compared to MLH1-a and MLH1-T5, which yield the targeted allele product of 198 bp. PCR was performed in a 25 μl reaction containing 100 ng of genomic DNA and 20 pmol of MLH1-T5 or MLH1-U and 40 pmol of MLH1-a, 0.2 mM of each dNTP, 1.5 mM $MgCl_2$ and 0.25 U of *Taq* Polymerase. Cycling conditions were 94 °C for 4 min, followed by 30 Cycles of 94 °C 1 min, 54 °C for 1 min, 72 °C 1 min. Extension in the last cycle was 72 °C for 3 min.

Antibodies and immunodetection. Antibody production and tests for specificity of Rad51 has been described[57]. The monoclonal antibody to MLH1 was produced by immunizing mice with a recombinant human Mlh1 fusion protein. Hybridoma clones were produced as described[58,59] and the antibodies purified from supernatants by protein G affinity chromatography. The immunochemical detection procedure was a modification[36] of the protocol of Moens *et al.*[60]. The preparations were incubated overnight at 4 °C with a monoclonal antibody (clone G168-15.3) against human MLH1 (diluted 1:400) and a polyclonal antibody against human RAD51 raised in rabbit[57] (diluted 1:200). The MLH1 antibody was detected with goat-anti-mouse-IgG conjugated with rhodamine (Pierce) and the RAD51 antibody with goat-anti-rabbit-IgG conjugated with fluorescein isothiocyanate (FITC, Sigma). All preparations were counter stained with 4',6-diaminino-2-phenylindole (DAPI). Preparations were examined and digitally imaged as described[36].

Western blot analysis. Culture of cells isolated from 15-day embryos is described elsewhere[16]. For Western blot analysis, protein from cultured cell extracts was resolved by SDS-PAGE, electro-blotted to Immobilion P transfer membrane (Millipore), and treated with Anti-MLH1 antibodies. Bound MLH1 antibody was detected by chemiluminescence (Renaissance, DuPont) using goat anti mouse IgG horseradish peroxidase conjugate (Pierce).

Histology of testis and ovary. Preparation of testis for histological analysis is described elsewhere[16]. All surrounding tissue was removed from the ovaries prior to overnight fixation in Zinc-buffered formalin. The fixed samples were embedded in paraffin wax, sectioned (4 μm), mounted and stained with either hematoxylin and esoin, or periodic acid, Schiff's and hematoxylin.

Single molecule PCR analysis. The PCR primers used for *D9Mit67* were as described[16]. Primers for amplification of locus *D1Mit355* in the first round were P1(5'–TGAAAAGAC-CTTTTCTCAAATAGTG–3') and P2(5'–CTTTGATTCT-GAAATATACAGCAA–3'). In the second round P2 was replaced with P3(5'–TAGGAACTGTTTTGTTGTTTTACAC–3'). The PCR buffer was described previously[35]. Volumes for first round reactions were 20 μl. From the first round 2 μl of product was added to 40 μl of PCR buffer for the second round. After an initial denaturation at 94 °C for 4 min, cycling conditions were for the first round of PCR an annealing step of 60 °C for 1 min (57 °C for *D1Mit355*), an extension step of 72 °C for 2 min and a denaturation step of 94 °C for 30 s (30 cycles). The second round of 25 cycles was identical for both loci and annealing and extension was carried out at 60 °C for 1.5 min. The last cycle of each round was an extension at 72 °C for 7 min.

Animals for Mlh1 localization. All normal mice were from the C57BL/6 inbred strain. Over 100 nuclei were imaged from 4 juvenile (18–21 days old) and 2 adult males, and over 150 nuclei were imaged from oocytes from 16–19 day old fetuses from 8 different litters. In addition, 50 nuclei were examined from an *Mlh1*-deficient mouse from a mixed 129/C57 genetic background. Surface spreads were prepared as described[36].

Acknowledgements

We thank B. Braun for advice on testis analysis, M. Matzuk for advice on ovarian pathology, R. Kolodner for human MLH1 intron/exon boundary information, and M. Robatzek and E. Regal for technical assistance. This work was supported by National Institutes of Health grants to R.M.L. (GM45413 and GM32741), T.A. (GM49779), N.A. (GM36745), and A.B. A.B. is an Associate Investigator with the Howard Hughes Medical Institute. S.M.B. received a fellowship from the C. G. Swebilius Fund, C.E.B. received an American Cancer Society fellowship and T.A.P. is a recipient of a Nation Science Foundation research fellowship in Biosciences Related to the Environment.

Received 21 March; accepted 20 May 1996.

1. Modrich, P. Mechanisms and biological effects of mismatch repair. *Annu. Rev. Genet.* **25**, 229–253 (1991).
2. Au, K.G., Welsh, K. & Modrich, P. Initiation of methyl-directed mismatch repair. *J. Biol. Chem.* **267**, 12142–12148 (1992).
3. Reenan, R.A.G. & Kolodner, R.D. Isolation and characterization of two *Saccharomyces cerevisiae* genes encoding homologs of the bacterial HexA and MutS mismatch repair proteins. *Genetics* **132**, 963–973 (1992).
4. Kramer, W., Kramer, B., Williamson, M.S. & Fogel, S. Cloning and nucleotide sequence of DNA mismatch repair gene *PMS1* from *Saccharomyces cerevisiae*: homology of PMS1 to procaryotic MutL and HexB. *J. Bacteriol.* **171**, 5339–5346 (1989).
5. Prolla, T., Christie, D.-M. & Liskay, R.M. Dual requirement in yeast DNA mismatch repair for MLH1 and PMS1, two homologs of the bacterial mutL gene. *Mol. Cell. Biol.* **14**, 407–415 (1994).
6. Bronner, C.E. *et al.* Mutation in the DNA mismatch repair gene homologue *hMLH1* is associated with hereditary nonpolyposis colon cancer. *Nature* **368**, 258–261 (1994).
7. Fishel, R.A. *et al.* The human mutator gene homolog MSH2 and its association with hereditary nonpolyposis colon cancer. *Cell* **75**, 1027–1038 (1993).
8. Leach, F.S. *et al.* Mutations of a mutS homolog in hereditary nonpolyposis colorectal cancer. *Cell* **75**, 1215–1225 (1993).
9. Papadopoulos, N. *et al.* Mutation of a mutL homolog in hereditary colon cancer. *Science* **263**, 1625–1629 (1994).
10. Nicolaides, N.C. *et al.* Mutations of two *PMS* homologues in hereditary nonpolyposis colon cancer. *Nature* **371**, 75–80 (1994).
11. New, L., Liu, K. & Crouse, G.F. The yeast gene *MSH3* defines a new class of eukaryotic MutS homologues. *Mol. Gen. Genet.* **239**, 97–108 (1993).
12. Marsischky, G.T., Filosi, N., Kane, M.F. & Kolodner, R. Redundancy of Saccharomyces cerevisiae MSH3 and MSH6 in MSH2-dependent mismatch repair. *Genes Dev.* **10**, 407–420 (1996).
13. Bishop, D.K., Andersen, J. & Kolodner, R.D. Specificity of mismatch repair following transformation of *Saccharomyces cerevisiae* with heteroduplex plasmid DNA. *Proc. Natl. Acad. Sci. USA* **86**, 3713–3717 (1989).
14. Williamson, M.S., Game, J.C. & Fogel, S. Meiotic gene conversion mutants in *Sacoharomyces cerevisiae*. I. Isolation and characterization of *pms1–1* and *pms1–2*. *Genetics* **110**, 609–646 (1985).
15. Prolla, T.A., Pang, Q., Alani, E., Kolodner, R.D. & Liskay, R.M. Interactions between the MSH2, MLH1 and PMS1 proteins during the initiation of DNA mismatch repair. *Science* **265**, 1091–1093 (1994).
16. Baker, S.M. *et al.* Male mice defective in the DNA mismatch repair gene PMS2 exhibit abnormal chromosome synapsis in meiosis. *Cell* **82**, 309–319 (1995).
17. Reitmair, A.H. *et al. MSH2* deficient mice are viable and susceptible to lymphoid tumours. *Nature Genet.* **11**, 64–70 (1995).
18. de Wind, N., Decker, M., Berns, A., Radman, M. & te Riele, H. Inactivation of the mouse MSH2 gene results in postreplication mismatch repair deficiency, methylation tolerance, hyperrecombination and predisposition to tumorigenesis. *Cell* **82**, 321–330 (1995).
19. Fishel, R., Ewel, A. & Lescoe, M.K. Purified human MSH2 protein binds to DNA containing mismatched nucleotides. *Cancer Res.* **54**, 5539–5542 (1994).
20. Li, G.-M. & Modrich, P. Restoration of mismatch repair to nuclear extracts of H6 colorectal tumor cells by a heterodimer of human MutL homologs. *Proc. Natl. Acad. Sci. USA* **92**, 1950–1954 (1995).
21. Petes, T.D., Malone, R.E. & Symington, L.S. Recombination in yeast. in *The Molecular and Cellular Biology of the Yeast Saccharomyces* vol. 1, (eds Broach, J., Jones, E. & Pringle, J.) 407–521 (Cold Spring Harbor Laboratory, Cold Spring Harbor, 1991).
22. Detloff, P., White, M.A. & Petes, T.D. Analysis of a gene conversion gradient at the *HIS4* locus in Saccharomyces cerevisiae. *Genetics* **132**, 113–123 (1992).
23. Alani, E., Reenan, R.A.G. & Kolodner, R. Interaction between mismatch repair and genetic recombination in Saccharomyces cerevisiae. *Genetics* **137**, 19–39 (1994).
24. Worth, L. Jr, Clark, S., Radman, M. & Modrich, P. Mismatch repair proteins MutS and MutL inhibit RecA-catalyzed strand transfer between diverged DNAs. *Proc. Natl. Acad. Sci. USA* **91**, 3238–3241 (1994).
25. Datta, A., Adjiri, A., New, L., Crouse, G.F. & Jinks-Robertson, S. Mitotic crossovers between diverged sequences are regulated by mismatch repair proteins in Saccharomyces cerevisiae. *Mol. Cell. Biol.* **16**, 1085–1093 (1996).
26. Petit, M.-A., Dimpfl, J., Radman, M. & Echols, H. Control of large chromosomal duplications in *Escherichia coli* by the mismatch repair system. *Genetics* **129**, 327–332 (1991).
27. Selva, E.M., New, L., Crouse, G.F. & Lahue, R.S. Mismatch correction acts as a barrier to homeologous recombination in Saccharomyces cerevisiae. *Genetics* **139**, 1175–1188 (1995).
28. Hunter, N., Chambers, S.R., Louis, E.J. & Borts, R.H. The mismatch repair system contributes to meiotic sterility in an interspecific yeast hybrid. *EMBO J.* **15**, 1726–1733 (1996).
29. Ross-Macdonald, P. & Roeder, G.S. Mutation of a meiosis-specific MutS homolog decreases crossing over but not mismatch correction. *Cell* **79**, 1069–1080 (1994).
30. Hollingsworth, N.M., Ponte, L. & Halsey, C. MSH5, a novel MutS homolog, facilitates meiotic reciprocal recombination between homologs in Saccharomyces cerevisiae but not mismatch repair. *Genes Dev.* **9**, 1728–1739 (1995).
31. Darlington, C.D. in *Recent Advances in Cytology*. (Churchill, London, 1937).
32. Hawley, R.S. Exchange and chromosomal segregation in eukaryotes. in *Meiosis* (eds Moens, P.B.) 497–527 (Academic Press, New York, 1987).
33. Carpenter, A.T. Gene conversion, recombination nodules, and the initiation of meiotic synapsis. *Bioessays* **6**, 232–236 (1987).
34. Ashley, T. Mammalian meiotic recombination: a reexamination. *Hum. Genet.* **94**, 587–593 (1994).
35. Leeflang, P.E., Hubert, R., Zhang, L. & Arnheim, N. Single sperm typing. in *Current Protocols in Human Genetics* vol. 1. (eds Dracopoli, N.C. *et al.*) 1.6.1–1.6.15 (John Wiley and Sons, New York, 1994).
36. Ashley, T. *et al.* Dynamic changes in Rad51 distribution on chromatin during meiosis in male and female vertebrates. *Chromosoma* **104**, 19–28 (1995).
37. Burgoyne, P.S. Genetic homology and crossing over in the X and Y chromosomes of mammals. *Hum. Genet.* **61**, 85–90 (1982).
38. Rouyer, F. *et al.* A gradient of sex linkage in the pseudoautosomal region of the human sex chromosomes. *Nature* **319**, 291–295 (1986).
39. Petit, C., Levilers, J. & Weissenbach, J. Physical mapping of the pseudoautosomal region: comparison with genetic linkage map. *EMBO J.* **7**, 2369–2379 (1988).
40. Rappold, G.A. & Lehrach, H. A long range restriction map of the pseudoautosomal region by partial digest PFGE analysis from the telomere. *Nucl. Acids Res.* **16**, 5361–5377 (1988).
41. Soriano, P. *et al.* High rate of recombination and double crossovers in the mouse pseudoautosomal region during male meiosis. *Proc. Natl. Acad. Sci. USA* **84**, 7218–7220 (1987).
42. Polani, P.E. & Jagiello, G.M. Chiasmata, meiotic univalents, and age in relation to aneuploid imbalance in mice. *Cytogenet. Cell Genet.* **16**, 505–529 (1976).
43. Moses, M.J. & Poorman, P.A. Synapsis, synaptic adjustment and DNA synthesis in mouse oocytes. in *Chromosomes Today* vol. 8. (eds Bennett, M.D., Gropp, A. & Wolf, U.) 90–103 (George Allen & Unwin, Boston, 1984).
44. Moses, M.J. Composition and role of the synaptonemal complex. *Symp. Soc. Exp. Biol.* **38**, 245–270 (1984).
45. Solari, A.J. Sex chromosome pairing and fertility in the heterogametic sex of mammals and birds. in *Fertility and Chromosome Pairing: Recent Studies in Plants and Animals* (eds Gillies, C.B.) 77–135 (CRC Press, Boca Raton, 1989).
46. Moses, M.J. Synaptonemal complex karyotyping in spermatocytes of the chinese hamster (Cricetulus). II. Morphology of the XY pair in spread preparations. *Chromosoma* **60**, 127–137 (1977).
47. Dietrich, A.J.J. & Mulder, P.J.P. A light and electron microscopic analysis of meiotic prophase in female mice. *Chromosoma* **88**, 377–385 (1983).
48. Dietrich, A.J.J. & Mulder, P.J.P. A light microscopic study of the development and behaviour of the synaptonemal complex in spermatocytes of the mouse. *Chromosoma* **83**, 409–418 (1981).
49. Goetz, P., Chandley, A.C. & Speed, R.M. Morphological and temporal sequence of meiotic prophase development at puberty in the male mouse. *J. Cell Science* **65**, 249–263 (1984).
50. Speed, R.M. Meiosis in the foetal mouse ovary. I. An analysis at the light microscope level using surface spreading. *Chromosoma* **85**, 427–437 (1982).
51. Roeder, G.S. Chromosome synapsis and genetic recombination: their roles in meiotic chromosome segregation. *Trends Genet.* **6**, 385–389 (1990).
52. West, S.C. Enzymes and molecular mechanisms of genetic recombination. *Annu. Rev. Biochem.* **61**, 603–640 (1992).
53. Jones, S.N., Roe, A.E., Donehower, L.A. & Bradley, A. Rescue of embryonic lethality in Mdm2-deficient mice by absence of p53. *Nature* **378**, 206–208 (1995).
54. Ramirez-Solis, R., Davis, A.C. & Bradley, A. Gene targeting in mouse embryonic stem cells. in *Guide to Techniques in Mouse Development* (eds Wassarman, P.M. & DePamhilis, M.L.) 855–878 (Academic, New York, 1993).
55. Bradley, A. Production and analysis of chimaeric mice. in *Teratocarcinomas and Embryonic Stem Cells: A Practical Approach.* (eds Robertson, E.J.) 113–151 (IRL, Oxford, 1987).
56. McMahon, A., P. & Bradley, A. The Wnt-1 (int-1) proto-oncogene is required for development of a large region of the mouse brain. *Cell* **62**, 1073–1085 (1990).
57. Haaf, T. *et al.* Nuclear foci of mammalian Rad51 recombination protein in somatic cells after DNA damage and it's localization in synaptonemal complexes. *Proc. Natl. Acad. Sci. USA* **92**, 2298–2302 (1995).
58. Galfre, G. *et al.* Antibodies to major histocompatibility antigens produced by hybrid cell lines. *Nature* **266**, 550–552 (1977).
59. de St. Groth, S.F. Monoclonal antibodies and how to make them. *Transplant. Proc.* **12**, 447–450 (1980).
60. Moens, P.B. *et al.* Synaptonemal complex antigen localization and conservation. *J. Cell Biol.* **105**, 93–103 (1987).